

Original Research Article

A Hydrodynamic Model of Flow in Bifurcating Streams, Part 2: Effects of Environmental Thermal Differentials

Abstract This paper presents a hydrodynamic model of flow in a bifurcating stream, in which the effects of environmental thermal differentials are investigated. The governing nonlinear and coupled equations are solved analytically using similarity transformation and perturbation series expansions methods. Solutions for the temperature, velocity and concentration are obtained and analyzed quantitatively and graphically. The results show that the heat exchange parameter reduces the velocity of the flow, and this enhances early deposition of the stream bed loads. Furthermore, it is seen that free convection force increases the flow velocity, thus serving as a cushion for the adverse effect of heat exchange parameter on the flow.

Keywords: *bifurcating stream, hydrodynamic model, thermal differentials, similarity transformation, perturbation method*

1. INTRODUCTION

Much of the studies on flow in streams and rivers have been carried out using non-hydrodynamic approaches such as hydrologic model, which involves the use of spatial form of the continuity equation or water balance and flux relation (see [1]); hydraulic model, which is based on the use of St. Venant equations (see [2]); stochastic probability model, which involves the use of Monte Carlo method (see [3, 4]). Being motivated by this, we presented an analytic and hydrodynamic model of the flow in a bifurcating stream. In the said model, which is part one of the study, the effects of bifurcation angle and nature of the source rocks on the flow were investigated, while the effects of environmental thermal differentials were played down. Presently, we are motivated to examine the situation where the environmental thermal differentials are considered significant. Therefore, the purpose of this study is to investigate the effect of environmental thermal differentials on the flow of a bifurcating stream.

Several reports exist in literature on the flow in bifurcating and non-bifurcating channels. Bifurcation phenomenon is seen in both natural and artificial worlds. Therefore, it is significant in science and engineering. This import greatly attracted the interest of researchers in the past decades. [5] introduced the use of theoretical approach or mathematical tools in the study of branching flows. [6] investigated a three-dimensional one-to-two symmetrical flow in which the mother is straight and of circular cross-section, containing a fully developed incident motion, while the diverging daughters are straight and of semi-circular cross-section. Using the method of direct numerical simulation and slender modeling for a variety of Reynolds number and divergent angles, they observed that there is a flow separation or reversal at the corners of the junction as well as the upstream and downstream influence with which the inlet pressure increases as the bifurcation angle increases. More so, [7] showed that changes in bifurcation angle alter the flow condition and changes the magnitude of the wall shear stress. [8] studied the flow phenomenon in micro/mini channel networks of symmetrical bifurcation using computer simulation with analytic validation, and saw that oscillation amplitude has dominant effects on the streaming velocity in channel networks. Moreso, they observed that the streaming velocity is proportional to the oscillation frequency. [9] studied blood flow in abifurcating artery, using the method of regular perturbation, and noticed that an increase in bifurcation angle and Reynolds number increases the transport velocity factor.

53

54 Furthermore, the flow through porous media is prevalent in nature and artificial settings.
55 Therefore it is of principal interest in science and engineering. It has relevance in petroleum
56 engineering for the study of the movement of natural gas, oil and water through the oil
57 reservoir; in chemical engineering for filtration of and purification processes; in hydrology
58 for studying the underground water resources. [10] Investigated the flow in a rotating porous
59 straight pipe, and showed that the Nusselt number increases with increase in porosity. [11]
60 studied the flow in a curved porous channel with rectangular cross-section filled with a fluid
61 saturated porous medium, the flow being driven by a constant azimuthal pressure gradient,
62 and using a generalized Fourier series method of solution found that the velocity profiles
63 depend on the geometry of the channel and Darcy number.

64

65 Moreso, the study of the flow of fluid through porous media has also been extended to
66 include the effect of magnetic field. [12] investigated the effect of magnetic field on the flow
67 in a rectangular enclosure using perturbation technique, and reported that the imposed
68 magnetic field diminished the wall shear. [13] examined the influence of magnetic field on
69 the skin friction factor of a steady fully developed laminar flow through a pipe experimentally
70 and by finite difference numerical scheme, and observed that the pressure drop varies in
71 proportion to the square of the magnetic field and sine angle; the pressure is proportional to
72 the flow rate, and the axial velocity asymptotically approaches its limit as the Hartmann
73 number becomes large. [14] studied the free convection flow through a vertical porous
74 channel in the presence of an applied magnetic field using the finite difference numerical
75 approach, and noticed that the velocity decreases with the increase in the magnetic and
76 porosity parameters throughout the region.

77

78 Similarly, magnetohydrodynamic convective heat and mass transfer in porous and non-
79 porous media is of considerable interest in technical field due to its applications in industries,
80 geothermal, high temperature plasma, liquid metal and MHD power generating systems. [15]
81 investigated the effects of magnetic field and convective force on the flow in bifurcating
82 porous fine capillaries using the regular perturbation series expansions method, and found
83 that magnetic field reduces the flow velocity, whereas the convective force increases it.
84 Moreso, [16] examined blood flow in bifurcating arteries analytically, and observed that an
85 increase in heat exchange parameter and Grashof number increases the velocity,
86 concentration and Nusselt number of the flow, while an increase in the heat exchange
87 parameter increases the Sherwood number.

88

89 The purpose of this present paper is to examine the effects of thermal differentials on a
90 bifurcating flowing stream.

91

92 The paper is organized in the following format: section 2 is the material and methods,
93 section 3 is the results and discussion, and section 4 is the conclusion.

94

95

96

2. MATERIAL AND METHODS

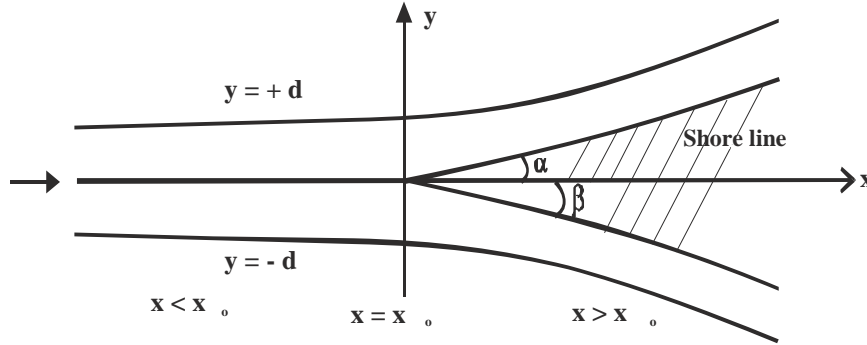
97

98 There is always a temperature difference between the internal/ambient temperature of the
99 stream and that at its surface called the external or environmental temperature condition.
100 This temperature differential can be described in terms of the Newton's law of cooling as

101 $\frac{\partial \theta}{\partial y} = h(\theta_{ext} - \theta_{int})$ where h is the film heat transfer coefficient which could be negative. The

102 magnitude of the temperature at the surface of the stream is influenced by the climatic
103 condition of the region where it is found. In particular, the environmental temperature

104 depends tremendously on the radiation from the sun. The higher the radiation the higher it
 105 becomes. When the environmental temperature is higher than the equilibrium temperature of
 106 the stream, heat flows from the surface into it, that is, the stream absorbs heat from the
 107 environmental source. The effects of heat absorption can be seen in the energization of the
 108 water particles.
 109
 110
 111



112
 113

114 Figure 1 A physical model of symmetrical bifurcating flowing stream (with $\alpha=\beta$, where α, β
 115 are the bifurcation angles).

116

117 We assume the stream bifurcates symmetrically as shown in Figure 1, and that the flow is
 118 axi-symmetrical about the z' -axis. Therefore, if (u', v') are respectively the velocity
 119 components of the fluid in the mutually orthogonal (x', y') axes, then the mathematical
 120 equations of mass balance/continuity, momentum, energy and diffusion governing the flow,
 121 considering the Boussinesq approximations, become:
 122

123
$$\frac{\partial u'}{\partial x'} + \frac{\partial v'}{\partial y'} = 0 \quad (1)$$

124
$$u' \frac{\partial u'}{\partial x'} + v' \frac{\partial u'}{\partial y'} = -\frac{1}{\rho'} \frac{\partial p'}{\partial x'} + \frac{\mu}{\rho'} \left(\frac{\partial^2 u'}{\partial x'^2} + \frac{\partial^2 u'}{\partial y'^2} \right) + g\beta_t (T' - T_\infty) + g\beta_c (C' - C_\infty)$$

125
$$-\frac{\sigma_e B_o^2 u'}{\rho'^2 \mu_m} - \frac{v u'}{\kappa} \quad (2)$$

126
$$u' \frac{\partial v'}{\partial x'} + v' \frac{\partial v'}{\partial y'} = -\frac{1}{\rho'} \frac{\partial p'}{\partial y'} + \frac{\mu}{\rho'} \left(\frac{\partial^2 v'}{\partial x'^2} + \frac{\partial^2 v'}{\partial y'^2} \right) \quad (3)$$

127
$$u' \frac{\partial T'}{\partial x'} + v' \frac{\partial T'}{\partial y'} = -\frac{1}{\rho'} \frac{k_o}{C_p} \left(\frac{\partial^2 T'}{\partial x'^2} + \frac{\partial^2 T'}{\partial y'^2} \right) + \frac{1}{\rho' C_p} Q (T' - T_\infty) \quad (4)$$

128
$$u' \frac{\partial C'}{\partial x'} + v' \frac{\partial C'}{\partial y'} = -\frac{D}{\rho'} \left(\frac{\partial^2 C'}{\partial x'^2} + \frac{\partial^2 C'}{\partial y'^2} \right) + \frac{k_r^2}{\rho'} (C' - C_\infty) \quad (5)$$

129 The model examines the dynamics of a bifurcating stream flowing from a point $x' = -\infty$
130 towards a shore at $x' = x_o$, then continued towards $x' = +\infty$, as seen in Figure 1. The
131 model shows that the channel is assumed to be symmetrical and divided into two regions:
132 the upstream (or mother) region $x' < x_o$ and downstream (or daughter) region $x' > x_o$,
133 where x_o is the bifurcation or the nodal point, which is assumed to be the origin such that
134 the stream boundaries become $y' = \pm d$ for the upstream region and $y' = \alpha x'$ for the
135 downstream region. Due to the geometrical transition between the mother and daughter
136 channels, the problem of wall curvature effect is bound to occur. To fix up this, a very simple
137 transition wherein the width of the daughter channel is made equal to half that of the mother
138 channel i.e. $\pm d$ is such that the variation of the bifurcation angle is straight-forwardly used
139 (see [6]). Furthermore, if the width of the stream ($2d$) is far less than its length (l_o) before
140 the point of bifurcation such that the ratio of $\frac{2d}{l_o} = \mathfrak{R} \ll 1$, (where \mathfrak{R} is the aspect ratio), the
141 flow is laminar and Poiseuille (see [17]). d is assumed to be non-dimensionally equal to one
142 (see [6]). Similarly, at the entry region of the mother channel, the flow velocity is given as
143 $u' = U_o(1 - y'^2)$, where U_o is the characteristic velocity, which is taken to be maximum at
144 the centre and zero at the wall (see [6]). Based on the fore-going, the boundary conditions
145 are:

$$146 \quad u' = 1, v' = 0, T' = 1, C' = 1 \quad \text{at } y' = 0 \quad (6)$$

$$147 \quad u' = 0, v' = 0, T' = T_w, C' = C_w \quad \text{at } y' = 1 \quad (7)$$

148 for the mother channel

$$149 \quad u' = 0, v' = 0, T' = 0, C' = 0 \quad \text{at } y' = 0 \quad (8)$$

$$150 \quad u' = 0, v' = 0, T' = \gamma_1 T_w, C' = \gamma_2 C_w, \gamma_1 < 1, \gamma_2 < 1 \quad \text{at } y' = \alpha x' \quad (9)$$

151 for the daughter channel

152 Introducing the dimensionless variables and similarity transformations,
153 we have

$$154 \quad f'' = 0 \quad (10)$$

$$155 \quad f''' + f'' - M_1^2 f' + \text{Re}(f' f'' + ff''') = -Gr \Theta - Gc \Phi \quad (11)$$

$$156 \quad \Theta'' + \Theta' + \text{Re Pr}(-f' \Theta' + f \Theta'') + N^2 \Theta = 0 \quad (12)$$

$$157 \quad \Phi'' + \Phi' + \text{Re Sc}(-f' \Phi' + f \Phi'') + \delta_1^2 \Phi = 0 \quad (13)$$

158 with the boundary indications:

$$159 \quad f = 1, f' = 0, \Theta = 1, \Phi = 1 \quad \text{at } \eta = 0 \quad (14)$$

$$160 \quad f' = 0, f = 0, \Theta = \Theta_w, \Phi = \Phi_w \quad \text{at } \eta = 1 \quad (15)$$

161 for the mother channel

$$162 \quad f = 0, f' = 0, \Theta = 0, \Phi = 0 \quad \text{at } \eta = 0 \quad (16)$$

163

167 $f' = 0, f = 0, \Theta = \gamma_1 \Theta_w, \Phi = \gamma_2 \Phi_w, \gamma_1 < 1, \gamma_2 < 1$ at $\eta = ax$ (17)

168

169 for the daughter channel

170 where

171 $M_1^2 = (\chi^2 + M^2)$

172 $x = \frac{x'}{\ell_c}, y = \frac{y'}{\ell_c}, u = \frac{u'}{U_o}, v = \frac{v'}{U_o}, p = \frac{p'}{p_\infty}, \rho = \rho' U_o^2, \Theta = \frac{T' - T_\infty}{T_w - T_\infty},$

173 $\Phi = \frac{C' - C_\infty}{C_w - C_\infty}, \nu = \frac{\rho}{\mu}, \text{Re} = \frac{\rho U_o \ell_c}{\mu}, \text{Gr} = \frac{\rho g \beta_t (T_w - T_\infty) \ell_c^2}{\mu U_o}, \text{Gc} = \frac{\rho g \beta_c (C_w - C_\infty)}{\mu U_o},$

174 $\chi^2 = \frac{\ell_c^2}{\kappa}, \delta_1^2 = \frac{k_r^2 \ell_c^2}{D}, M^2 = \frac{\sigma_e B_o^2 \ell_c^2}{\rho \mu \mu_m}, N^2 = \frac{Q \ell_c^2}{k_o}, \text{Sc} = \frac{\mu}{\rho D},$

175

176 are the dimensionless variables,

177 $\Psi = (U_o \nu x)^{1/2} f(\eta), \eta = \left(\frac{U_o}{\nu x} \right)^{1/2} y$ (18)

178 the similarity transformations,

179 $u = \frac{\partial \Psi}{\partial y}, v = -\frac{\partial \Psi}{\partial x}$ (19)

180 the velocity components,

181

182 and β_t and β_c are the volumetric expansion coefficient for temperature and concentration

183 respectively; p' is the pressure; C_∞ is the concentration at equilibrium; T_∞ is the

184 temperature at equilibrium; κ is the permeability parameter of the porous medium; B_o^2 is the

185 applied uniform magnetic field strength due to the nature of the fluid; σ_e is the electrical conductivity

186 of the fluid; k_o is the thermal conductivity of the fluid; C_p is the specific heat capacity at constant

187 pressure; Q is the heat absorption coefficient; k_r^2 is the rate of chemical reaction of the fluid, which

188 is homogeneous and of order one; C' is concentration (quantity of material being transported); D

189 diffusion coefficient; \mathbf{g} is gravitational field vector; T' is the fluid temperature; ρ' is the density of

190 the fluid; μ is the viscosity of the fluid; μ_m is the magnetic permeability of the fluid; ν is the

191 kinematic viscosity; ℓ_c is the scale length; U_o is the characteristic or reference velocity which

192 is maximum at the centre and almost zero at the wall; C_w is the constant wall concentration

193 at which the channel is maintained; T_w is the constant wall temperature at which the

194 channel is maintained; p_∞ is the ambient/equilibrium pressure; Re is the Reynolds number;

195 Gr is the Grashof number due to temperature difference; Gc is the Grashof number due to

196 concentration difference; χ^2 is the local Darcy number; M^2 is the Hartmann's number; Pr is

197 the Prandtl number; Sc is the Schmidt number; δ_1^2 is the rate of chemical reaction; and N^2 is

198 the heat exchange parameter.

199

200 Equations (10) - (13) are coupled and highly non-linear. Therefore, to linearize and make
 201 them tractable, we introduce the regular perturbation series solutions of the form:

202
 203
$$h(x, y) = h_o(x, y) + \xi h_1(x, y) + \dots \quad (20)$$

 204

205 where $\xi = \frac{1}{Re} \ll 1$ is the perturbing parameter. We choose this parameter because,
 206 almost at the point of bifurcation, due to a change in the geometrical configuration, the
 207 inertial force rises and the momentum increases. The increase in the momentum is
 208 associated with a drastic increase in the Reynolds number, indicating a sort of turbulent flow.
 209 In this regard, equations (10) - (17) become:

210
 211 for the zeroth order:

212
$$f_o'' = 0 \quad (21)$$

213
$$f_o'''' + f_o'' - M_1^2 f_o' = -Gr\Theta_o - Gc\Phi_o \quad (22)$$

214
$$\Theta_o'' + \Theta_o' + N^2\Theta_o = 0 \quad (23)$$

215
$$\Phi_o'' + \Phi_o' + \delta_1^2\Phi_o = 0 \quad (24)$$

216 with the boundary conditions

217
$$f_o = 1, f_o' = f_o'' = 0, \Theta_o = 1, \Phi_o = 1 \text{ at } \eta = 0 \quad (25)$$

218
$$f_o = 0, f_o' = f_o'' = 0, \Theta_o = \Theta_w, \Phi_o = \Phi_w \text{ at } \eta = 1 \quad (26)$$

219 for the first order:

220
$$f_1'' = 0 \quad (27)$$

221
$$f_1'''' + f_1'' - M_1^2 f_1' = f_o' f_o'' - f_o f_o''' - Gr\Theta_1 - Gc\Phi_1 \quad (28)$$

222
$$\Theta_1'' + \Theta_1' + N^2\Theta_1 = Pr(f_o' \Theta_o' - f_o \Theta_o'') \quad (29)$$

223
$$\Phi_1'' + \Phi_1' + \delta_1^2\Phi_1 = Sc(f_o' \Phi_o' - f_o \Phi_o'') \quad (30)$$

224 with the boundary conditions

225
$$f_1 = 0, f_1' = 0, \Theta_1 = 0, \Phi_1 = 0 \text{ at } \eta = 0 \quad (31)$$

226
$$f_1 = 0, f_1' = 0, \Theta_1 = \gamma_1\Theta_w, \Phi_1 = \gamma_2\Phi_w, \gamma_1 < 1, \gamma_2 < 1 \text{ at } \eta = ax \quad (32)$$

227

228 The zeroth order equations describe the flow in the upstream channel, while the first order
 229 equations describe the flow in the downstream channels. The presence of the zeroth order
 230 terms in the first order equations indicate the influence of the upstream on the downstream
 231 flow.

232

233 The solutions to equations (21) - (26) and (27) - (32) are:

234

235
$$\Theta_o(\eta) = \frac{\Theta_w e^{\frac{1}{2}(1-\eta)} \sinh \mu_1 \eta}{\sinh \mu_1} + \frac{e^{-\frac{1}{2}(1-\eta)} \sinh \mu_1 (1-\eta)}{\sinh \mu_1} \quad (33)$$

236

237
$$\Phi_o(\eta) = \frac{\Phi_w e^{\frac{1}{2}(1-\eta)} \sinh \mu_2 \eta}{\sinh \mu_2} + \frac{e^{-\frac{1}{2}(1-\eta)} \sinh \mu_2 (1-\eta)}{\sinh \mu_2} \quad (34)$$

238

$$f_o(\eta) = \frac{(f_{o(p)}(0)e^{-(\mu_3+\eta/2)} \sinh \mu_3 \eta)}{\sinh \mu_3} + \frac{(f_{o(p)}(1)e^{-1/2(1-\eta)} \sinh \mu_3 \eta)}{\sinh \mu_3} - f_{o(p)}(0)e^{-(\mu_3+\eta/2)} + f_{o(p)}(\eta) \quad (35)$$

240

241

242 for the mother channel

243

244

$$\Theta_1(\eta) = \frac{\gamma_1 \Theta_w e^{\frac{1}{2}(\alpha x - \eta)} \sinh \mu_1 \eta}{\sinh(\mu_1 \alpha x)} - \frac{\Theta_{1(p)}(\alpha x) e^{-\frac{1}{2}(\alpha x - \eta)} \sinh \mu_1 \eta}{\sinh(\mu_1 \alpha x)} + \frac{\Theta_{1(p)}(0) e^{-(\mu_1 \alpha x + \eta/2)} \sinh \mu_1 \eta}{\sinh(\mu_1 \alpha x)} - \Theta_{1(p)}(0) e^{-(\alpha x - (\mu_1 + 1/2)\eta)} + \Theta_{1(p)}(\eta) \quad (36)$$

246

247

248

$$\Phi_1(\eta) = \frac{\gamma_2 \Phi_w e^{\frac{1}{2}(\alpha x - \eta)} \sinh \mu_2 \eta}{\sinh(\mu_2 \alpha x)} + \frac{\Phi_{1(p)}(\alpha x) e^{-\frac{1}{2}(\alpha x - \eta)} \sinh \mu_2 \eta}{\sinh(\mu_2 \alpha x)} + \frac{\Phi_{1(p)}(0) e^{-(\mu_2 \alpha x + \eta/2)} \sinh \mu_2 \eta}{\sinh(\mu_2 \alpha x)} - \Phi_{1(p)}(0) e^{-(\alpha x - (\mu_2 + 1/2)\eta)} + \Phi_{1(p)}(\eta) \quad (37)$$

250

251

252

$$f_1(\eta) = \frac{f_{1(p)}(0) e^{-(\mu_3 \alpha x + \eta/2)} \sinh \mu_3 \eta}{\sinh \mu_3 \alpha x} + \frac{f_{1(p)}(\alpha x) e^{1/2(\alpha x - \eta)} \sinh \mu_3 \eta}{\sinh(\mu_3 \alpha x)}$$

254

255

$$-f_{1(p)}(0) e^{(\alpha x - (\mu_3 + 1/2)\eta)} + f_{1(p)}(\eta) \quad (38)$$

256

257 and for the daughter region.

258

259 3 RESULTS AND DISCUSSION

260

261 **This paper investigates** the effects of thermal differentials on the flow in a bifurcating stream.
 262 To this end, Figure2 – Figure 8 obtained using Maple 12 computational software show the
 263 profiles of the flow variables obtained for various values of χ_1^2 , N^2 and Gr/Gc . For realistic
 264 values of $Pr = 0.71$, $\gamma_1 = 0.6$, $\gamma_2 = 0.6$, $\gamma = 0.7$, $\Phi_w = 2.0$, $\Theta_w = 2.0$, $\delta_1^2 = 0.2$, $M^2 = 0.2$, $\alpha = 10$,
 265 $Re = 400$, and for varying values of $\chi^2 = 0.1, 0.5, 1.0, 10$; $N^2 = 0.001, 0.01, 0.1, 0.4$ and
 266 $Gr/Gc = 0.01, 0.1, 0.5, 1.0, 5, 10$ the profiles indicate that the flow velocity decreases as χ^2
 267 and N^2 increase, but increases with the increase in Gr/Gc .
 268

269 A high porosity of the stream bank may give room for a soak-away of the water. Therefore,
 270 as the porosity increases the stream water is soaked away into its bank, thus leading to a
 271 decrease in its volume. Moreover, the water level of the stream will remain decreased if there
 272 is not a commensurate increase in the water supplied from the aquifers that feed it, possibly,
 273 due to man's water delivery activities on them. Consequently, the flow velocity,
 274 which is usually maximum when the volume is high, decreases. These may account for what
 275 is seen in Figure 2. And, this is in perfect agreement with [11] and [14]. In another
 276 development, a high porosity of the source rock of the stream creates room for water to flow
 277 from the supplying aquifers into it. However, by the analysis of this model the flow velocity of
 278 the water from the aquifers decreases with high porosity of the source rock. Even so, the
 279 oscillatory/fluctuation motion, manifested in the form of back-and-forth movement of the
 280 water, as seen in Figure 3 and Figure 4, possibly, seems to be partly due to the internal
 281 waves developed in the water in the flow process, or may be due to the interaction between
 282 the pressure force and the gravity force. This is an account from wave theory.

283
284
285
286
287
288
289
290
291
292
293
294
295
296
297
298
299
300
301

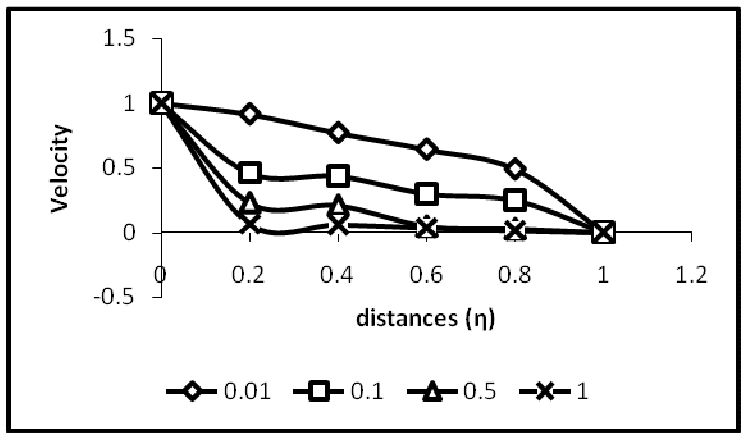


Figure 2 Velocity-positivity parameter (χ^2) profiles at various distances (η) in the mother channel

302
303
304

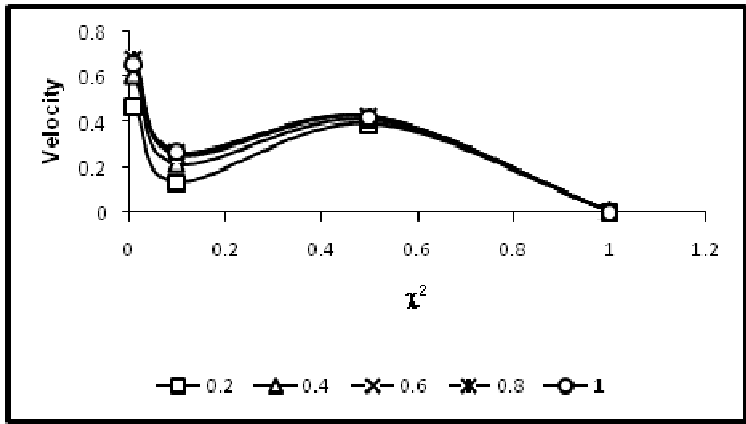
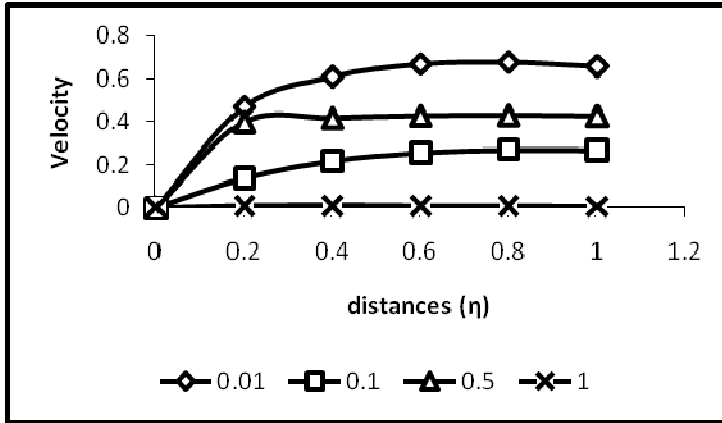


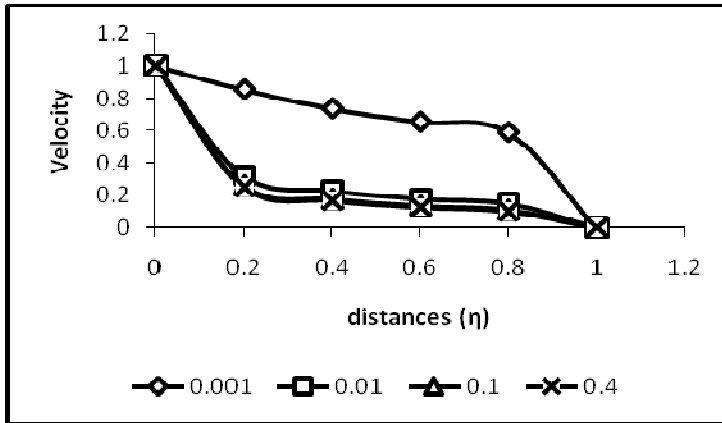
Figure 3 Velocity profiles for various porosity parameter (χ^2) in the daughter channel



305
306
307
308
309
310
311
312
313
314
315

Figure 4 Velocity-velocity parameter (χ^2) profiles at various distances (η) in the daughter channel

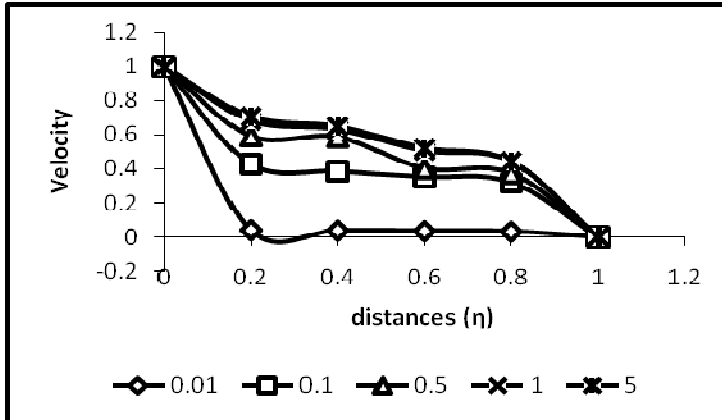
Furthermore, as the environmental temperature increases, the stream may lose its water through evaporation, and soak-away into the dry flood plain. This leads to a decrease in its water level. Again, if the water supplied from the aquifers is not equatable to that which is lost (due to man's water delivery activities on them), the stream water level in such a season remains reduced. Consequently, the velocity which is usually maximum when the water volume is high, drops. This accounts for the results seen in Figure 5.



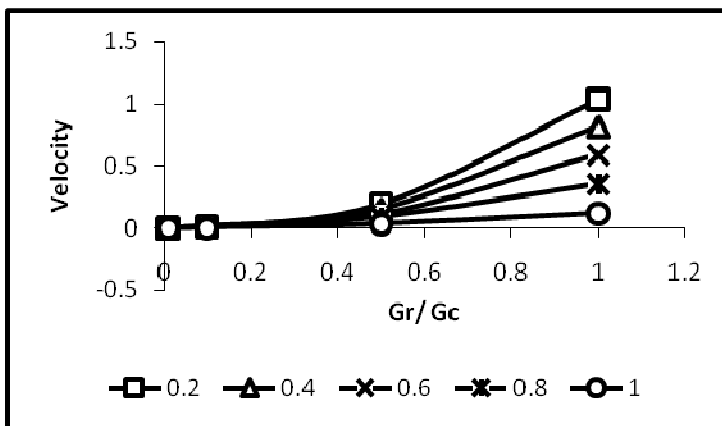
316
317
318
319
320
321
322
323
324
325
326
327
328
329
330
331

Figure 5 Velocity-heat exchange parameter (N^2) profiles at various distances (η) in the mother channel

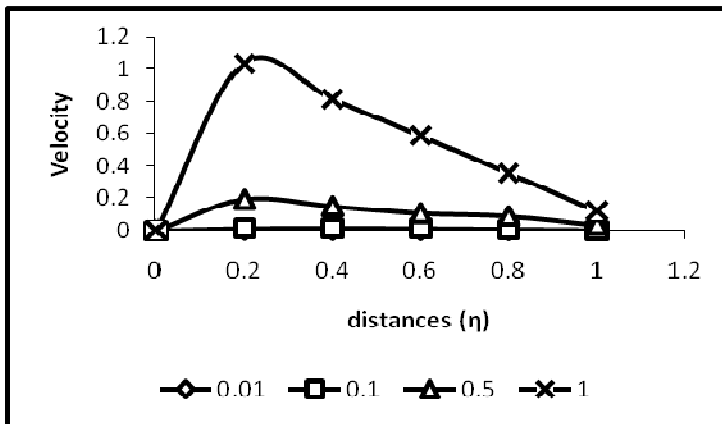
On the other hand, there is always a temperature differential between the environmental temperature and the ambient temperature of the water. The temperature differential in the presence of gravity produces free convection currents, which serve as lifting/buoyancy forces for the water particles. In particular, the temperature differential depends on the environmental temperature, which in turn depends on the radiation from the sun. The higher the radiation, the higher the temperature differential, and the higher the convection currents, otherwise called buoyancy force or Grashof number (which in this case is due to temperature change) produced. The increase in the buoyancy force increases the flow velocity (see Figure 6 –Figure 8). A comparison with previous research works shows a complete agreement, see [15] and [16].



332
333 Figure 6 Velocity-Grashof number (Gr/G_c) profiles at various distances (η) in the mother
334 channel.
335



336
337 Figure 7 Velocity profiles for various Grashof numbers (Gr/G_c) in the daughter channel
338



339
340 Figure 8 Velocity-Grashof numbers (Gr/G_c) profiles at various distances (η) in the daughter
341 channel
342

343
344 The increase and decrease in the velocity, coupled with the oscillating/fluctuating motion of
345 the water have some great significance on the flow. The increase in velocity saves the
346 stream from early shallow-up as it tends to delay the deposition of the sediments and bed

347 loads it is carrying in its course towards the standing water bodies into which it empties its
348 water. On the other hand, the decrease in velocity produces the contrary situation.
349 Furthermore, the oscillatory/fluctuating motion leads to loss of energy for the flow in the axial
350 direction, and this also adversely affects the transport of the bedloads.

351

352 **4 CONCLUSION**

353

354 The steady flow in a bifurcating stream with emphasis on the effects of environmental
355 thermal differentials is presented. The solutions of the problem are analyzed graphically. The
356 analyses show that the porosity and heat exchange parameters decrease the flow velocity,
357 while the free convection force increases it. Furthermore, an increase in the porosity leads to
358 a fluctuating motion. These results have serious implications on the flow. The increase in
359 velocity tends to delay the deposition of sediments/bed loads on the stream floor and flood
360 plains, thus saving it from early shallow-up. On the other hand, the decrease in the velocity
361 leads to the contrary. Similarly, the fluctuating motion leads to loss of energy for the axial
362 flow. In particular, the free convection force tends to cushion the velocity reducing-effects of
363 porosity and heat exchange parameters. It is worthy to note that a considerable amount of
364 work is needed to further study and understand the streaming flow hydrodynamically.

365

366 **REFERENCES**

367

368 [1] Singh VP. Hydrologic systems: volume 1, Rainfall-run-off modeling. New Jersey: Prentice
369 House Englewood Cliffs; 1988.

370 [2] Singh VP. Kinematic wave modeling in water resources, surface water hydrology. New
371 York: John Wiley and Sons; 1996.

372 [3] Hoey T. Temporal variations in bed load transport rate and sediment storage in gravel-
373 bed rivers. Prog. Physical Geography. 1992; 16(3): 319–38.

374 [4] Marusic Galino. A study on the mathematical modeling of water quality in river-type
375 aquatic system. WSEAS Transactions on Fluid Mechanics. 2013; 80–9.

376 [6] Pedley TJ, Schroter RC, Sudlow MF. The prediction of pressure drop and variation of
377 resistance within the human bronchial airways. Resp. Physiology. 1970; 9: 387–405.

378 [7] Tadjfar M, Smith FT. Direct simulation and modeling of a 3-dimensional bifurcating tube
379 flow. J Fluid Mechanics. 2004; 519:1-32.

380 [8] Soulis. J Biomech. 2004; 39:742–49.

381 [9] Zhang Z, Fadl A, Liu C, Meyer DML. Fluid streaming in micro/mini-bifurcating networks. J
382 Fluid Engineering, ASME. 2009; 131: 084501-8.

383 [10] Okuyade WIA, Abbey TM. Analytic study of blood flow in bifurcating arteries, part 1-
384 effects of bifurcating angle and magnetic field. International Organization of Scientific
385 Research J Mathematics. 2015. I.D: G54040 - in press

386 [11] Rao Ramana VV, Sobha VV. Heat transfer of a saturated porous flow in a rotating
387 straight pipe. Proceeding of the Tenth National Heat and Mass Transfer Conference,
388 Madurai Kamaraj University, Madurai. 1987; 13.

389 [12] Avramenko AA, Kuznetsov AV. Flow in a curved porous channel with rectangular cross-
390 section. J Porous Media. 2008; 241-48. Doi: 10.1615/JporMedia.v.11.i3.20

391 [13] Asadolah, Malekzadeh, Amir Heydarinasab, Bahram Dabir. Magnetic field effect on
392 fluid flow characteristics in a pipe for laminar flow. J Mechanical Sci. and Tech. 2011;
393 25:333-39.

394 [14] Venkateswalu S, Suryanarayama Rao KV, Rambupal Reddy B. Finite difference
395 analysis on convective heat transfer flow through porous medium in a vertical channel with
396 magnetic field, Indian Journal of Applied Maths and Mechanics. 2011; 7(7):74–94.

397 [15] Okuyade WIA. MHD blood flow in bifurcating porous fine capillaries. African J Science
398 Research. 2015; 4(4): 56-59.

399 [16] Okuyade WIA, Abbey TM. Analytic study of blood flow in bifurcating arteries, part 2-
 400 effects of environmental temperature differentials. International Organization of Scientific
 401 Research J Mechanical Engineering. 2015. I.D: G54083 - in press
 402 [17] A.R. Bestman. Global models for the biomechanics of green plants, part 1. International
 403 J Energy Research. 1991; 16: 677– 84.

404
 405
 406
 407
 408

APPENDICES

$$409 \quad f_{o(p)}(\eta) = - \left(\frac{n_3}{n_3(n_3^2 - n_2n_3)} - \frac{1}{(n_3^2 - n_2n_3)} \right) \left(\frac{GrAe^{\lambda_1\eta}}{\lambda_1} + \frac{GrBe^{\lambda_2\eta}}{\lambda_2} + \frac{GrCe^{m_1\eta}}{m_1} + \frac{GrDe^{m_2\eta}}{m_2} \right)$$

410
 411

$$412 \quad + \frac{n_3}{n_3(n_3^2 - n_2n_3)} \left(\frac{GrAe^{\lambda_1\eta}}{(\lambda_1 - n_2)} + \frac{GrBe^{\lambda_2\eta}}{(\lambda_2 - n_2)} + \frac{GrCe^{m_1\eta}}{(m_1 - n_2)} + \frac{GrDe^{m_2\eta}}{(m_2 - n_2)} \right)$$

413

$$414 \quad - \frac{1}{n_3(n_3^2 - n_2n_3)} \left(\frac{GrAe^{\lambda_1\eta}}{(\lambda_1 - n_3)} + \frac{GrBe^{\lambda_2\eta}}{(\lambda_2 - n_3)} + \frac{GrCe^{m_1\eta}}{(m_1 - n_3)} + \frac{GrDe^{m_2\eta}}{(m_2 - n_3)} \right)$$

415

$$416 \quad \lambda_1 = -\frac{1}{2} + \frac{\sqrt{1-4N^2}}{2}, \lambda_2 = -\frac{1}{2} - \frac{\sqrt{1-4N^2}}{2}$$

$$417 \quad \lambda_1 = -\frac{1}{2} + \mu_1, \lambda_2 = -\frac{1}{2} - \mu_1, \mu_1 = \frac{\sqrt{1-4N^2}}{2}$$

$$418 \quad m_1 = -\frac{1}{2} + \mu_2, m_2 = -\frac{1}{2} - \mu_2, \mu_2 = \frac{\sqrt{1-4\delta_1^2}}{2}$$

$$419 \quad n_2 = -\frac{1}{2} + \mu_3, n_3 = -\frac{1}{2} - \mu_3, \mu_3 = \frac{\sqrt{1-4M^2}}{2}$$

$$A = \frac{\Theta_w e^{1/2} - e^{\mu_1}}{\sinh \mu_1}, B = \frac{e^{\mu_1} - \Theta_w e^{1/2}}{\sinh \mu_1}, C = \frac{\Phi_w e^{1/2} - e^{\mu_2}}{\sinh \mu_2}, D = \frac{e^{\mu_2} - \Phi_w e^{1/2}}{\sinh \mu_2}$$

420
 421

$$\Theta_{1(p)}(\eta) = \frac{Pr}{(\lambda_2 - \lambda_1)} \left[\lambda_1 F A e^{(\lambda_1 + n_2)\eta} + \lambda_1 G A e^{(\lambda_1 + n_3)\eta} \right]$$

422

$$- \left(\frac{n_3}{n_2(n_3^2 - n_2n_3)} - \frac{1}{(n_3^2 - n_2n_3)} \right) \left(\frac{GrA^2 e^{2\lambda_1\eta}}{\lambda_2} + \frac{\lambda_1 GrABe^{(\lambda_1 + \lambda_2)\eta}}{\lambda_2} + \frac{\lambda_1 GcACE^{(\lambda_1 + m_1)\eta}}{m_1} + \frac{\lambda_1 GcADE^{(\lambda_1 + m_2)\eta}}{m_2} \right)$$

423

$$424 \quad + \frac{n_3}{n_2(n_3^2 - n_2n_3)} \left(\frac{\lambda_1 GrA^2 e^{2\lambda_1\eta}}{(\lambda_1 - n_2)} + \frac{\lambda_1 GrABe^{(\lambda_1 + \lambda_2)\eta}}{(\lambda_2 - n_2)} + \frac{\lambda_1 GcACe^{(\lambda_1 + m_1)\eta}}{(m_1 - n_2)} + \frac{\lambda_1 GcADe^{(\lambda_1 + m_2)\eta}}{(m_2 - n_2)} \right)$$

425

$$426 \quad - \frac{1}{(n_3^2 - n_2n_3)} \left(\frac{\lambda_1 GrA^2 e^{2\lambda_1\eta}}{(\lambda_1 - n_3)} + \frac{\lambda_1 GrABe^{(\lambda_1 + \lambda_2)\eta}}{(\lambda_2 - n_3)} + \frac{\lambda_1 GcACe^{(\lambda_1 + m_1)\eta}}{(m_1 - n_3)} + \frac{\lambda_1 GcADe^{(\lambda_1 + m_2)\eta}}{(m_2 - n_3)} \right)] +$$

427

428

$$\Phi_{1(p)}(\eta) = \frac{Sc}{(m_2 - m_1)} [m_1 F C e^{(m_1 + n_2)\eta} + m_1 G C e^{(m_1 + n_3)\eta}$$

$$429 \quad - \left(\frac{n_3}{n_2(n_3^2 - n_2n_3)} - \frac{1}{(n_3^2 - n_2n_3)} \right) \left(\frac{m_1 GrACe^{(\lambda_1 + m_1)\eta}}{\lambda_1} + \frac{m_1 GrBCe^{(\lambda_2 + m_1)\eta}}{\lambda_2} + GcC^2 e^{2m_1\eta} \right. \\ \left. + \frac{m_1 GcCDe^{(m_1 + m_2)\eta}}{m_2} \right)$$

430

$$431 \quad + \frac{n_3}{n_2(n_3^2 - n_2n_3)} \left(\frac{m_1 GrACe^{(\lambda_1 + m_1)\eta}}{(\lambda_1 - n_2)} + \frac{m_1 GrBCe^{(\lambda_2 + m_1)\eta}}{(\lambda_2 - n_2)} + \frac{m_1 GcC^2 e^{2m_1\eta}}{(m_1 - n_2)} + \frac{m_1 GcCDe^{(m_1 + m_2)\eta}}{(m_2 - n_2)} \right)$$

432

433

$$434 \quad - \frac{1}{(n_3^2 - n_2n_3)} \left(\frac{m_1 GrACe^{(\lambda_1 + m_1)\eta}}{(\lambda_1 - n_3)} + \frac{m_1 GrBCe^{(\lambda_2 + m_1)\eta}}{(\lambda_2 - n_3)} + \frac{m_1 GcC^2 e^{2m_1\eta}}{(m_1 - n_3)} + \frac{m_1 GcCDe^{(m_1 + m_2)\eta}}{(m_2 - n_3)} \right)]$$

435

436

$$437 \quad - Gr \left\{ \frac{J_1 e^{n_1\eta}}{n_2} + \frac{J_2 e^{n_2\eta}}{n_2} + \frac{Pr}{(\lambda_2 - \lambda_1)} \left[\frac{\lambda_1 F A e^{(\lambda_1 + n_2)\eta}}{(\lambda_1 + n_2)} + \frac{\lambda_1 G A e^{(\lambda_1 + n_3)\eta}}{(\lambda_1 + n_3)} \right] \right.$$

438

$$439 \quad \left. - \left(\frac{n_3}{(n_3^2 - n_2n_3)} - \frac{1}{(n_3^2 - n_2n_3)} \right) \left(\frac{GrA^2 e^{2\lambda_1\eta}}{2} + \frac{GrBAe^{(\lambda_1 + \lambda_2)\eta}}{(\lambda_1 + \lambda_2)} + \frac{\lambda_1 GcCAe^{(\lambda_1 + m_1)\eta}}{(\lambda_1 + m_1)m_1} + \frac{\lambda_1 GcDAe^{(\lambda_1 + m_2)\eta}}{(\lambda_1 + m_2)m_2} \right) \right.$$

440

441

$$442 \quad + \frac{n_3}{n_2(n_3^2 - n_2n_3)} \left(\frac{GrA^2 e^{2\lambda_1\eta}}{2(\lambda_1 - n_2)} + \frac{\lambda_1 GrBAe^{(\lambda_1 + \lambda_2)\eta}}{(\lambda_2 - n_2)(\lambda_1 + \lambda_2)} + \frac{\lambda_1 GcCAe^{(\lambda_1 + m_1)\eta}}{(m_1 - n_2)(\lambda_1 + m_1)} + \frac{\lambda_1 GcDAe^{(\lambda_1 + m_2)\eta}}{(m_2 - n_2)(\lambda_1 + m_2)} \right)$$

443

444

$$445 \quad -\frac{1}{(n_3^2 - n_2 n_3)} \left(\frac{GrA^2 e^{2\lambda_1 \eta}}{2(\lambda_1 - n_3)} + \frac{\lambda_1 GrBAe^{(\lambda_1 + \lambda_2)\eta}}{(\lambda_2 - n_3)(\lambda_1 + \lambda_2)} + \frac{\lambda_1 GcCAe^{(\lambda_1 + m_1)\eta}}{(m_1 - n_3)(\lambda_1 + m_1)} + \frac{\lambda_1 GcDAe^{(\lambda_1 + m_2)\eta}}{(m_2 - n_3)(\lambda_1 + m_2)} \right)]$$

446 + ...}

447

448

$$449 \quad f_{1(p)}(\eta) = \left(\frac{n_3}{n_2(n_3^2 - n_2 n_3)} - \frac{1}{(n_3^2 - n_2 n_2)} \right) \left\{ [Fe^{n_2 \eta} + Ge^{n_3 \eta} \right.$$

450

$$451 \quad - \left(\frac{n_3}{n_2(n_3^2 - n_2 n_3)} - \frac{1}{(n_3^2 - n_2 n_3)} \right) \left(\frac{GrAe^{\lambda_1 \eta}}{\lambda_1} + \frac{GrBe^{\lambda_2 \eta}}{\lambda_2} + \frac{GcCe^{m_1 \eta}}{m_1} + \frac{GcDe^{m_2 \eta}}{m_2} \right)$$

$$452 \quad + \frac{n_3}{n_2(n_3^2 - n_2 n_3)} \left(\frac{GrAe^{\lambda_1 \eta}}{(\lambda_1 - n_2)} + \frac{GrBe^{\lambda_2 \eta}}{(\lambda_2 - n_2)} + \frac{GcCe^{m_1 \eta}}{(m_1 - n_2)} + \frac{GcDe^{m_2 \eta}}{(m_2 - n_2)} \right)$$

453

$$454 \quad - \frac{1}{(n_3^2 - n_2 n_3)} \left(\frac{GrAe^{\lambda_1 \eta}}{(\lambda_1 - n_3)} + \frac{GrBe^{\lambda_2 \eta}}{(\lambda_2 - n_3)} + \frac{GcCe^{m_1 \eta}}{(m_1 - n_3)} + \frac{GcDe^{m_2 \eta}}{(m_2 - n_3)} \right)] + \dots$$

455

$$456 \quad - \frac{1}{(n_3^2 - n_2 n_3)} \left(\frac{GrAe^{\lambda_1 \eta}}{(\lambda_1 - n_3)} + \frac{GrBe^{\lambda_2 \eta}}{(\lambda_2 - n_3)} + \frac{GcCe^{m_1 \eta}}{(m_1 - n_3)} + \frac{GcDe^{m_2 \eta}}{(m_2 - n_3)} \right)]$$

457

$$458 \quad - \left(\frac{n_3}{(n_3^2 - n_2 n_3)} - \frac{1}{(n_3^2 - n_2 n_3)} \right) \left(\frac{GrA^2 e^{2\lambda_1 \eta}}{2} + \frac{GrBAe^{(\lambda_1 + \lambda_2)\eta}}{(\lambda_1 + \lambda_2)} + \frac{\lambda_1 GcCAe^{(\lambda_1 + m_1)\eta}}{(\lambda_1 + m_1)m_1} + \frac{\lambda_1 GcDAe^{(\lambda_1 + m_2)\eta}}{(\lambda_1 + m_2)m_2} \right)$$

459

460

$$461 \quad + \frac{n_3}{n_2(n_3^2 - n_2 n_3)} \left(\frac{GrA^2 e^{2\lambda_1 \eta}}{2(\lambda_1 - n_2)} + \frac{\lambda_1 GrBAe^{(\lambda_1 + \lambda_2)\eta}}{(\lambda_2 - n_2)(\lambda_1 + \lambda_2)} + \frac{\lambda_1 GcCAe^{(\lambda_1 + m_1)\eta}}{(m_1 - n_2)(\lambda_1 + m_1)} + \frac{\lambda_1 GcDAe^{(\lambda_1 + m_2)\eta}}{(m_2 - n_2)(\lambda_1 + m_2)} \right)$$

462

463

$$464 \quad - \frac{1}{(n_3^2 - n_2 n_3)} \left(\frac{GrA^2 e^{2\lambda_1 \eta}}{2(\lambda_1 - n_3)} + \frac{\lambda_1 GrBAe^{(\lambda_1 + \lambda_2)\eta}}{(\lambda_2 - n_3)(\lambda_1 + \lambda_2)} + \frac{\lambda_1 GcCAe^{(\lambda_1 + m_1)\eta}}{(m_1 - n_3)(\lambda_1 + m_1)} + \frac{\lambda_1 GcDAe^{(\lambda_1 + m_2)\eta}}{(m_2 - n_3)(\lambda_1 + m_2)} \right)]$$

465

$$467 \quad + \dots - Gc \left\{ \frac{R_1 e^{m_1 \eta}}{m_1} + \frac{R_2 e^{m_2 \eta}}{m_2} + \frac{Sc}{(m_2 - m_1)} \left[\frac{m_1 Fc e^{(m_1 + n_2)\eta}}{(m_1 + n_2)} + \frac{m_1 Gc e^{(m_1 + n_3)\eta}}{(m_1 + n_3)} \right] + \right.$$

468

$$469 \left(\frac{n_3}{n_2(n_3^2 - n_2 n_3)} - \frac{1}{(n_3^2 - n_2 n_3)} \right) \left(\frac{m_1 GrACe^{(m_1 + \lambda_1)\eta}}{\lambda_1(m_1 + \lambda_1)} + \frac{m_1 GrBCe^{(m_1 + \lambda_1)\eta}}{\lambda_2(m_1 + \lambda_1)} + \frac{GcC^2 e^{2m_1\eta}}{2m_1} + \frac{m_1 GcDCe^{(m_1 + m_2)\eta}}{m_2(m_1 + m_2)} \right)$$

470
471

$$472 - \frac{n_3}{n_2(n_3^2 - n_2 n_3)} \left(\frac{m_1 GrACe^{(m_1 + \lambda_1)\eta}}{(\lambda_1 - n_2)(m_1 + \lambda_1)} + \frac{m_1 GrBCe^{(m_1 + \lambda_2)\eta}}{(\lambda_2 - n_2)(m_1 + \lambda_2)} + \frac{GcC^2 e^{2m_1\eta}}{(m_1 - n_2)^2} + \frac{m_1 GcDCe^{(m_1 + m_2)\eta}}{(m_2 - n_2)(m_1 + m_2)} \right)$$

473
474

$$475 - \frac{1}{(n_3^2 - n_2 n_3)} \left(\frac{m_1 GrACe^{(m_1 + \lambda_1)\eta}}{(\lambda_1 - n_3)(m_1 + \lambda_1)} + \frac{m_1 GrBCe^{(m_1 + \lambda_2)\eta}}{(\lambda_2 - n_3)(m_1 + \lambda_2)} + \frac{GcC^2 e^{2m_1\eta}}{(m_1 - n_3)^2} + \frac{m_1 GcDCe^{(m_1 + m_2)\eta}}{(m_2 - n_3)(m_1 + m_2)} \right)]$$

476 + ...]
477

$$478 E = 0 \quad F = \frac{(f_{o(p)}(0)e^{-(\mu_3 + 1/2)} - f_{o(p)}(1))e^{1/2}}{2 \sinh \mu_3},$$

479

$$480 G = \frac{-(f_{o(p)}(0)e^{-(\mu_3 + 1/2)} - f_{o(p)}(1))e^{1/2}}{2 \sinh \mu_3} - f_{o(p)}(0)$$

$$481 J_1 = \frac{e^{\alpha x/2} (\gamma_1 \Theta_w - \Theta_{1(p)}(\alpha x) + \Theta_{1(p)}(0)e^{-(\mu_1 + 1/2)\alpha x})}{2 \sinh(\mu_1 \alpha x)},$$

$$482 J_2 = \frac{-e^{\alpha x/2} (\gamma_1 \Theta_w - \Theta_{1(p)}(\alpha x) + \Theta_{1(p)}(0)e^{-(\mu_1 + 1/2)\alpha x})}{2 \sinh(\mu_1 \alpha x)} - \Theta_{1(p)}(0)$$

$$483 R_1 = \frac{e^{\alpha x/2} (\gamma_2 \Phi_w - \Phi_{1(p)}(\alpha x) + \Phi_{1(p)}(0)e^{-(\mu_2 + 1/2)\alpha x})}{2 \sinh(\mu_2 \alpha x)},$$

484

$$485 R_2 = \frac{-e^{\alpha x/2} (\gamma_2 \Phi_w - \Phi_{1(p)}(\alpha x) + \Phi_{1(p)}(0)e^{-(\mu_2 + 1/2)\alpha x})}{2 \sinh(\mu_2 \alpha x)} - \Phi_{1(p)}(0)$$